A REDUNDANT AIRCRAFT ATTITUDE SYSTEM BASED ON MINIATURISED GYRO CLUSTERS DATA FUSION BY USING KALMAN FILTERING

Ioana Raluca EDU[1], Teodor Lucian GRIGORIE[2], Andreea-Cătălina ENACHE[3], Florin ANCUȚA[4], Costin CEPIȘCĂ[5]

The paper presents a redundant strap-down attitude system which uses three miniaturized gyro sensors linear clusters in the detection unit. The data from the sensors in each of the three clusters are fused by using a Kalman filter, in order to improve the useful angular speed signal measured by the detection unit. In the paper are successively exposed the data fusion algorithm and the theoretical background of the attitude system. Finally, is shown the Matlab/Simulink software implementation and experimental validation of the redundant inertial attitude system.

Keywords: Strap-down inertial navigation system, redundant attitude system, data fusion, Kalman filtering, experimental validation

1. Introduction

By using theories and calculations related to inertial navigation systems, the corresponding data for the movement of a vehicle as position, velocity and attitude are obtained. In the simple case of mono-dimensional movement, inertial navigation technique consists in the measurement the total acceleration on board of the vehicle followed by its numerical integration, in order to determine the vehicle speed and position relative to the initial point. On the other way, in aeronautics, inertial navigation systems (INS), besides the speed and position of the vehicle have to provide to the pilot information related to the aircraft attitude relative to the local horizontal plane, in terms of yaw, roll and pitch angles. Also, all the avionics systems, the autopilots, the navigation system and the weapons system, are based on a correct and accurate calculation of these angles. Therefore, to monitor the aircraft movement in a three-dimensional space by using such an inertial technique, two basis information are needed: the linear acceleration and the angular speed of the moving vehicle relative to the navigation frame, considered as inertial for the developed application. The used instruments used for

[1] Faculty of Electrical Engineering, University POLITEHNICA of Bucharest, Romania,e-mail: edu_ioana_raluca@yahoo.com
[2] Faculty of Electrical Engineering, University of Craiova, Romania, e-mail: lgrigore@elth.ucv.ro,
[3] Faculty of Electrical Engineering, University POLITEHNICA of Bucharest, Romania
[4] Faculty of Electrical Engineering, University POLITEHNICA of Bucharest, Romania
[5] Faculty of Electrical Engineering, University POLITEHNICA of Bucharest, Romania

the acceleration and angular speed detection are accelerometers, and gyros, respectively [1]-[8].

In a simplified manner, the INS theory consists in the next three steps: 1) Once angular speed detected, by using an inertial attitude system the attitude angles are calculated and the Direction Cosine Matrix (DCM) relating the vehicle and navigation frames is estimated; 2) The measured linear acceleration components in vehicle frame are converted in navigation frame by using the currently estimated DCM; and 3) The new obtained values of the vehicle linear acceleration in navigation frame are numerically integrated and, based on the initial values of the vehicle speed and position, its current speed and position are obtained. In reality, the things are a little beat complicated due to the errors appearing in the system, which necessitate special numerical algorithms for estimation and compensation. The positioning errors with INS result from the partial knowledge of the initial conditions, from the inertial system's numerical calculus and from gyros and accelerometers errors. Whatever the cause of the inertial sensor errors, the result is parasitizing of the useful signal obtained from the sensor output, signal that is then provided to the navigator.

The gyro sensors errors, firstly reflected in the measured values of the angular speed components, have a bigger impact both at the level of rotation movement and at a level of translation movement monitoring, while the acceleration sensors errors, reflected in the measured values of acceleration components, are visible only at the translation movement level [1]-[10]. The gyro sensors errors, firstly reflected in the measured values of the angular speed components, have a bigger impact both at the level of rotation movement and at a level of translation movement monitoring. The acceleration sensors errors, reflected in the measured values of acceleration components, are visible only at the translation movement level [1]-[10]. In other words, the inertial sensors' accuracy has a main role in the navigation system's precision.

From the point of view of the sensors, the INS have evolved from the low accuracy, electro-mechanical inertial sensors that guided the first V2 rockets, to the solid-state sensors of today, built in MEMS (micro-electro-mechanical sensors), NEMS (nano-electro-mechanical sensors), MOEMS (micro-opto-electro-mechanical sensors) or NOEMS (nano-opto-electro-mechanical sensors) technologies. Thus, for many applications, the oversized and expensive classical inertial measurement units (IMU) were replaced with low-cost and low-dimensions ones. Unfortunately, these size and cost related advantages, brought by the miniaturized inertial sensors, were impaired by the obtaining of poor performance in terms of noise density, bias and scale factor stabilities [11]-[17].

Because of the spectral overlapping of the noise generated by the inertial sensors with the frequencies considered as a part of the real movement of the monitored vehicle, the sensors output signal filtering under the 100 Hz frequencies is not recommended [4]-[6]. The actual researches in the domain are looking for different methods to remove or limit this noise, by using or not of another navigation system which aid the INS, the statistical methods having the largest impact on this study achievement [1]-[8]. Following these research tendencies in the field, our research team started a project which aims to develop some high-precision strap-down inertial navigators, based on the connection and adaptive integration of the nano and micro inertial sensors in low cost networks, with a high degree of redundance. In this way, were conceived and implemented software some algorithms to statistically fuse the data from miniaturized inertial sensors, organized in redundant networks, in order to obtain high performance and redundant IMUs. In the current phase, the project activities focus to the integration of the developed sensors data fusion algorithms with different types of inertial navigators IMUs.

This paper presents such a redundant strap-down inertial attitude system based on miniaturized gyros clusters data fusion by using Kalman filtering.

2. Data fusion algorithm

The presented data fusion algorithm is based on the idea of building redundant linear clusters of miniaturized gyro sensors in the same attitude system of the inertial navigator, followed by each gyro cluster data fusion with a Kalman filter. The resulted structure provides to the inertial navigator the advantage to have a redundant attitude system in terms of gyro detection unit, and, in the same time, offers a significant improvement of the angular speed detection accuracy. Such a redundant cluster of sensors supposes the mounting of several gyro sensors on each of the three axis of the strap-down detection unit in the navigator as in Fig. 1.

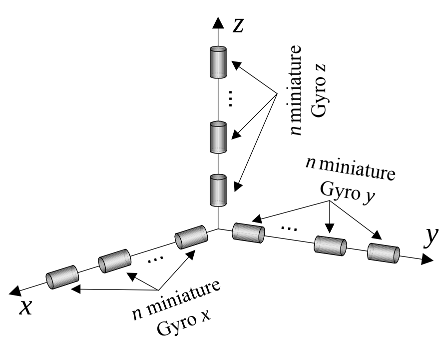

Fig. 1. Redundant structure of the attitude system containing three gyros clusters

The data fusion algorithm was proposed and presented by the authors in the paper at the reference [18]. According to its generalized form, each of the three used gyro sensors linear clusters contains n collinear sensors, which provide independent estimates $z_i \; (i = \overline{1,n})$ of the same angular speed x applied on respective axis. The n independent measures $z_i \; (i = \overline{1,n})$, obtained from the gyro sensors, are object of the sensors internal errors, and are characterized by the $\sigma_i^2 \; (i = \overline{1,n})$ variances.

According to [18], if x is considered to be the system-state desired to be estimated, then the filter should give an $\hat{x}$ estimate of the x quantity starting from the system' equations:

$$\underbrace{[x_k]}_{(1\times 1)} = \underbrace{[x_{k-1}]}_{(1\times 1)} + \underbrace{[w_k]}_{(1\times 1)}, \tag{1}$$

$$\underbrace{\begin{bmatrix} z_{1k} \\ \cdots \\ z_{ik} \\ \cdots \\ z_{nk} \end{bmatrix}}_{[z_k]\,(n\times 1)} = \underbrace{\begin{bmatrix} 1 \\ \cdots \\ 1 \\ \cdots \\ 1 \end{bmatrix}}_{[H_k]\,(n\times 1)} \cdot \underbrace{[x_k]}_{(1\times 1)} + \underbrace{\begin{bmatrix} \nu_{1k} \\ \cdots \\ \nu_{ik} \\ \cdots \\ \nu_{nk} \end{bmatrix}}_{[\nu_k]\,(n\times 1)}, \; i = \overline{1,n}. \tag{2}$$

$[w_k]$ and $[\nu_k]$ are uncorrelated zero-mean Gaussian white noise characterizing the process noise, respectively the measurement noise, and having the normal probability distributions given by equations

$$p([w_k]) \sim N(0,[Q_k]), \;\; p([\nu_k]) \sim N(0,[R_k]); \tag{3}$$

$[Q_k]$ and $[R_k]$ are the covariance matrices of the two noises.

The associated Kalman fusion algorithm is given with the expressions [18]:

1) Time update

- *a priori* state estimate:

$$\underbrace{[\hat{x}_k^-]}_{(1\times 1)} = \underbrace{[\hat{x}_{k-1}]}_{(1\times 1)}, \tag{4}$$

- *a priori* estimate covariance:

$$\underbrace{[P_k^-]}_{(1\times 1)} = \underbrace{[P_{k-1}]}_{(1\times 1)} + \underbrace{[Q_k]}_{(1\times 1)}, \tag{5}$$

2) Measurement update:

- optimal Kalman gain:

$$\underbrace{[K_k]}_{(1\times n)} = \underbrace{[P_k^-]}_{(1\times 1)} \cdot \underbrace{[H_k^T]}_{(1\times n)} \cdot \{\underbrace{[H_k]}_{(n\times 1)} \cdot \underbrace{[P_k^-]}_{(1\times 1)} \cdot \underbrace{[H_k^T]}_{(1\times n)} + \underbrace{[R_k]}_{(n\times n)}\}^{-1}, \tag{6}$$

- *a posteriori* state estimate:

$$\underbrace{[\hat{x}_k]}_{(1\times 1)} = \underbrace{[\hat{x}_k^-]}_{(1\times 1)} + \underbrace{[K_k]}_{(1\times n)} \cdot \{\underbrace{[z_k]}_{(n\times 1)} - \underbrace{[H_k]}_{(n\times 1)} \cdot \underbrace{[\hat{x}_k^-]}_{(1\times 1)}\}, \tag{7}$$

- *a posteriori* estimate covariance:

$$\underbrace{[P_k]}_{(1\times 1)} = \{1 - \underbrace{[K_k]}_{(1\times n)} \cdot \underbrace{[H_k]}_{(n\times 1)}\} \cdot \underbrace{[P_k^-]}_{(1\times 1)}, \tag{8}$$

The Kalman gain matrix has the expression:

$$[K_k] = [K_{1k} \quad \cdots \quad K_{ik} \quad \cdots \quad K_{nk}],\ i = \overline{1,n}, \tag{9}$$

and, because the measures $z_1, z_2, ..., z_n$ are independent and the noises $\nu_i\ (i = \overline{1,n})$ are uncorrelated, the $[R_k]$ matrix results with the form:

$$[R_k] = \begin{bmatrix} \sigma_{1k}^2 & \cdots & 0 & \cdots & 0 \\ \cdots & \cdots & \cdots & \cdots & \cdots \\ 0 & \cdots & \sigma_{ik}^2 & \cdots & 0 \\ \cdots & \cdots & \cdots & \cdots & \cdots \\ 0 & \cdots & 0 & \cdots & \sigma_{nk}^2 \end{bmatrix},\ i = \overline{1,n}. \tag{10}$$

It is very well known that the quality of the estimation procedure in the Kalman filter strongly depends by the priori noise statistics quality. Usually, the Kalman filter formulation assumes complete a priori knowledge of the process and measurement noise covariance matrices $[Q_k]$ and $[R_k]$. In our application we estimated firstly the process noise covariance matrix $[Q_k]$ and used continuously the obtained value, while for the measurement noise covariance matrix $[R_k]$ we proposed a method to be on-line dynamically adjusted. In this way, we used a buffer in order to have data for each gyro cluster in repeated frames format. If *m* is the number of samples provided by each of the *n* gyro sensors in a second, then by using a FIFO (first in first out) buffer we generated data frames of *m* consecutive samples. Also, we established that two consecutive generated data frames should be superposed with (*m*-1) samples. For each data frame, the variances of the independent measures $z_i\ (i = \overline{1,n})$ were calculated with equations:

$$\sigma_i^2(k) = \sigma_{ik}^2 = \frac{1}{m}\sum_{k=1}^{m}[z_i(k) - \bar{z}_i(k)]^2 = \frac{1}{m}\sum_{k=1}^{m}[z_{ik} - \bar{z}_{ik}]^2,\ i = (\overline{1,n}), \tag{11}$$

where: $z_i(k) = z_{ik}$ is the k^{th} measure from the i^{th} gyro sensor and corresponds to the k^{th} data frame; $\sigma_i^2(k) = \sigma_{ik}^2$ is the variance of the measure z_i for the k^{th} data frame and will be used in "data fusion" for the next data frame; $\bar{z}_i(k) = \bar{z}_{ik}$ is the arithmetic mean of the m samples acquired from the i^{th} gyro sensor in the k^{th} data frame.

The data fusion algorithm block diagram can be organized as in Fig. 2.

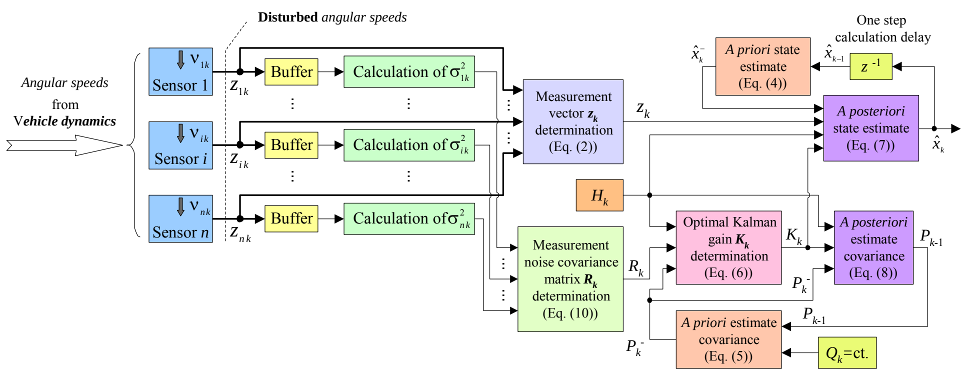

Fig. 2. Block diagram of the data fusion algorithm

3. Attitude system theoretical background

As we already stated, the determination of an aircraft flight attitude by using inertial techniques involves the determination of the roll, pitch and yaw angles from the navigation data acquired from a gyro triad. The actual inertial navigation systems use the strap-down configuration, having the advantage of miniaturization, which makes it ideal for use in all types of applications vis-à-vis of the other inertial technique based on the using of a gyro-stabilized platform. From the point of view of strap-down architecture, two methods for determining the attitude are known: the attitude quaternion method and the matrix method. However, both of them lead in the end to the achievement of the attitude matrix characterizing the transition between the vehicle frame and the navigation frame. Obtaining the final attitude matrix involves the numerical integration of the differential Poisson attitude equation, in one of its two forms, the matrix or the quaternionic one [1]-[8].

The two attitude representations are absolutely equivalent, but the numerical integration of the quaternionic form has several advantages related to the presence of only four parameters linked by a single constraint condition in the ortho-normalization process, compared with the matrix parameterization, which involves the presence of nine parameters bound by three orthogonality conditions and three normality conditions. Moreover, the attitude matrix ortho-normalization involves the existence of an iterative algorithm, which complicates to some degree the numerical calculation. Therefore, the usual recourse is made to the numerical integration of the Poisson quaternionic attitude equation [19]. The attitude system inputs are the values of the angular speed components $\omega_x, \omega_y, \omega_z$ measured using the strap-down gyro triad and the initial values of the roll, pitch and yaw angles. In the numerical attitude algorithm both the attitude quaternion and the DCM R_l^v, that switches between the local horizontal frame and the vehicle frame, are involved. The quaternionic differential Poisson attitude equation to be integrated has the form [1]-[8], [19], [20]:

$$\dot{Q} = \frac{1}{2}\begin{bmatrix} 0 & \omega_z & -\omega_y & \omega_x \\ -\omega_z & 0 & \omega_x & \omega_y \\ \omega_y & -\omega_x & 0 & \omega_z \\ -\omega_x & -\omega_y & -\omega_z & 0 \end{bmatrix}\begin{bmatrix} q_1 \\ q_2 \\ q_3 \\ q_0 \end{bmatrix}; \tag{12}$$

q_0, q_1, q_2 and q_3 are the components of the attitude quaternion Q. After Wilcox ([19], [20]), the new values of these components (at the time t_{n+1}) are derived from theirs past values (at the time t_n) by using the next equation:

$$\begin{bmatrix} q_1 \\ q_2 \\ q_3 \\ q_0 \end{bmatrix}_{t_{n+1}} = \begin{bmatrix} C_m & S_m\Delta\phi_z(t_n) & -S_m\Delta\phi_y(t_n) & S_m\Delta\phi_x(t_n) \\ -S_m\Delta\phi_z(t_n) & C_m & S_m\Delta\phi_x(t_n) & S_m\Delta\phi_y(t_n) \\ S_m\Delta\phi_y(t_n) & -S_m\Delta\phi_x(t_n) & C_m & S_m\Delta\phi_z(t_n) \\ -S_m\Delta\phi_x(t_n) & -S_m\Delta\phi_y(t_n) & -S_m\Delta\phi_z(t_n) & C_m \end{bmatrix}\begin{bmatrix} q_1 \\ q_2 \\ q_3 \\ q_0 \end{bmatrix}_{t_n}, \tag{13}$$

where C_m, S_m are the m-order development coefficients of the Wilcox algorithm (Table 1 [19], [20]). The angular increments of the roll, pitch and yaw axes ($\Delta\phi_x$, $\Delta\phi_y$, $\Delta\phi_z$) in equation (13) are calculated with the relations:

$$\begin{aligned} \Delta\phi_x(t_n) &= \int_{t_n}^{t_{n+1}} \omega_x(t_n)\mathrm{d}t = \omega_x(t_n)(t_{n+1}-t_n) = \omega_x(t_n)\Delta t, \\ \Delta\phi_y(t_n) &= \int_{t_n}^{t_{n+1}} \omega_y(t_n)\mathrm{d}t = \omega_y(t_n)(t_{n+1}-t_n) = \omega_y(t_n)\Delta t, \\ \Delta\phi_z(t_n) &= \int_{t_n}^{t_{n+1}} \omega_z(t_n)\mathrm{d}t = \omega_z(t_n)(t_{n+1}-t_n) = \omega_z(t_n)\Delta t, \end{aligned} \tag{14}$$

which consider that the gyro readings $\omega_x, \omega_y, \omega_z$ are constant over a time integration step $\Delta t = t_{n+1} - t_n$. Also, the norm ϕ_0, which characterizes the total angular increment over a time integration step and influences the C_m and S_m coefficients values, results with the equation:

$$\phi_0(t_n) = \sqrt{\Delta\phi_x^2(t_n) + \Delta\phi_y^2(t_n) + \Delta\phi_z^2(t_n)}. \quad (15)$$

As a consequence, the expressions of the new attitude quaternion components are:

$$\begin{aligned}
q_1(t_{n+1}) &= C_m q_1(t_n) + S_m\Delta\phi_z(t_n)q_2(t_n) - S_m\Delta\phi_y(t_n)q_3(t_n) + S_m\Delta\phi_x(t_n)q_0(t_n),\\
q_2(t_{n+1}) &= -S_m\Delta\phi_z(t_n)q_1(t_n) + C_m q_2(t_n) + S_m\Delta\phi_x(t_n)q_3(t_n) + S_m\Delta\phi_y(t_n)q_0(t_n),\\
q_3(t_{n+1}) &= S_m\Delta\phi_y(t_n)q_1(t_n) - S_m\Delta\phi_x(t_n)q_2(t_n) + C_m q_3(t_n) + S_m\Delta\phi_z(t_n)q_0(t_n),\\
q_0(t_{n+1}) &= -S_m\Delta\phi_x(t_n)q_1(t_n) - S_m\Delta\phi_y(t_n)q_2(t_n) - S_m\Delta\phi_z(t_n)q_3(t_n) + C_m q_0(t_n).
\end{aligned} \quad (16)$$

Due to the numerical truncation, the new obtained attitude quaternion doesn't respect the ortho-normalization condition. Therefore, an ortho-normalization step is required. According to the literature ([1]-[8], [19], [20]) the new quaternion components values respecting the ortho-normalization condition may be calculated with the equations:

$$q_{1ortho}(t_{n+1}) = \frac{q_1(t_{n+1})}{|Q(t_{n+1})|},\ q_{2ortho}(t_{n+1}) = \frac{q_2(t_{n+1})}{|Q(t_{n+1})|},\ q_{3ortho}(t_{n+1}) = \frac{q_3(t_{n+1})}{|Q(t_{n+1})|},\ q_{0ortho}(t_{n+1}) = \frac{q_0(t_{n+1})}{|Q(t_{n+1})|}, \quad (17)$$

where the norm $|Q(t_{n+1})|$ results from equation:

$$|Q(t_{n+1})| = \sqrt{q_0^2(t_{n+1}) + q_1^2(t_{n+1}) + q_2^2(t_{n+1}) + q_3^2(t_{n+1})}. \quad (18)$$

Table 1

Coefficients of the Wilcox algorithm

m	C_m	S_m
1	1	1/2
2	$1-\phi_0^2/8$	1/2
3	$1-\phi_0^2/8$	$1/2-\phi_0^2/48$
4	$1-\phi_0^2/8+\phi_0^4/384$	$1/2-\phi_0^2/48$
5	$1-\phi_0^2/8+\phi_0^4/384$	$1/2-\phi_0^2/48+\phi_0^4/3840$
6	$1-\phi_0^2/8+\phi_0^4/384-\phi_0^6/46080$	$1/2-\phi_0^2/48+\phi_0^4/3840$

Based on the equivalence between attitude quaternion and R_l^v matrix ([1]-[8], [19], [20]), the new values of the R_l^v matrix elements result as follow:

$$
\begin{aligned}
r_{11}(t_{n+1}) &= q_0^2(t_{n+1}) + q_1^2(t_{n+1}) - q_2^2(t_{n+1}) - q_3^2(t_{n+1}),\\
r_{12}(t_{n+1}) &= 2[q_1(t_{n+1})q_2(t_{n+1}) + q_0(t_{n+1})q_3(t_{n+1})],\\
r_{13}(t_{n+1}) &= 2[q_1(t_{n+1})q_3(t_{n+1}) - q_0(t_{n+1})q_2(t_{n+1})],\\
r_{21}(t_{n+1}) &= 2[q_1(t_{n+1})q_2(t_{n+1}) - q_0(t_{n+1})q_3(t_{n+1})],\\
r_{22}(t_{n+1}) &= q_0^2(t_{n+1}) + q_2^2(t_{n+1}) - q_1^2(t_{n+1}) - q_3^2(t_{n+1}),\\
r_{23}(t_{n+1}) &= 2[q_3(t_{n+1})q_2(t_{n+1}) + q_0(t_{n+1})q_1(t_{n+1})],\\
r_{31}(t_{n+1}) &= 2[q_1(t_{n+1})q_3(t_{n+1}) + q_0(t_{n+1})q_2(t_{n+1})],\\
r_{32}(t_{n+1}) &= 2[q_2(t_{n+1})q_3(t_{n+1}) - q_0(t_{n+1})q_1(t_{n+1})],\\
r_{33}(t_{n+1}) &= q_0^2(t_{n+1}) + q_3^2(t_{n+1}) - q_1^2(t_{n+1}) - q_2^2(t_{n+1}).
\end{aligned}
\tag{19}
$$

From this point, hawing in mind the expressions of the R_l^v matrix elements as functions of the attitude angles, derived from a three successive rotations operation (e.g. yaw with angle ψ, pitch with angle θ and roll with angle φ) ([1]-[8], [19], [20]):

$$
\begin{aligned}
r_{11} &= \cos\theta\cos\psi,\\
r_{12} &= \cos\theta\sin\psi,\\
r_{13} &= -\sin\theta,\\
r_{21} &= \sin\varphi\sin\theta\cos\psi - \cos\varphi\sin\psi,\\
r_{22} &= \sin\varphi\sin\theta\sin\psi + \cos\varphi\cos\psi,\\
r_{23} &= \sin\varphi\cos\theta,\\
r_{31} &= \cos\varphi\sin\theta\cos\psi + \sin\varphi\sin\psi,\\
r_{32} &= \cos\varphi\sin\theta\sin\psi - \sin\varphi\cos\psi,\\
r_{33} &= \cos\varphi\cos\theta.
\end{aligned}
\tag{20}
$$

Result the roll, pitch and yaw angles with the formulas ([1]-[8], [19], [20]):

$$
\begin{aligned}
\varphi(t_{n+1}) &= \mathrm{arctg}[r_{23}(t_{n+1})/r_{33}(t_{n+1})],\\
\theta(t_{n+1}) &= \arcsin[-r_{13}(t_{n+1})],\\
\psi(t_{n+1}) &= \mathrm{arctg}[r_{12}(t_{n+1})/r_{11}(t_{n+1})].
\end{aligned}
\tag{21}
$$

4. Software implementation and experimental validation of the redundant inertial attitude system

The presented attitude algorithm was implemented software by using an S-function in the Matlab/Simulink package. The S-function includes also the ortho-normalisation algorithm as well as the initialisation procedure of the method.

For an easiest communication of the user with the algorithm, a Graphical User Interface was built (Fig. 3). It allows the user to set the initial values of the attitude angles (Initial roll angle, Initial pitch angle, and Initial yaw angle) in degrees and the sample time. Also, at the interface level, the user can choose the truncation order of the numerical method used to integrate the Poisson equation (m=1 to 6). The interface masks the Simulink block "Attitude" (Fig. 4. a), which implements our algorithm. In fact, this is the first layer block, having as inputs the angular speeds (ω_{xv}, ω_{yv}, ω_{zv}) read by the gyro triad and expressed in degrees/s, and as outputs the attitude angles (roll - φ, pitch - θ, and yaw - ψ) expressed in degrees. At the next layer level (second layer), the block "Attitude" contains „Attitude L2" block (Fig. 4. b), implementing the algorithm S-function (Fig. 4. c).

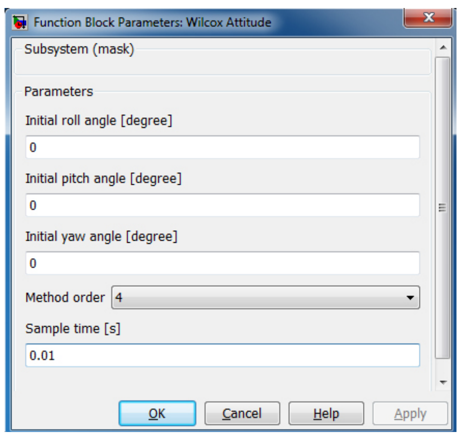

Fig. 3. Graphical User Interface of the algorithm

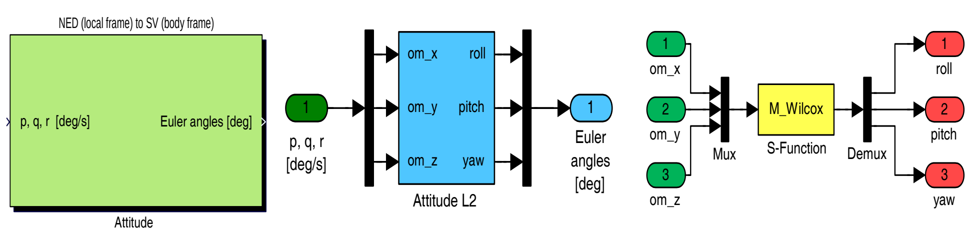

a b c

Fig. 4. Simulink block "Attitude"

The model in Fig. 4 implements only the algorithm processing the data obtained from the sensors unit, i.e. gyro triad. In order to develop the entire inertial attitude system in the redundant proposed variant, the data fusion algorithm model for each of the three channels should be inserted between the gyro sensors and the model in Fig. 4. As a consequence, starting from the mathematics of the data fusion algorithm (equations (1) to (11)) organized as in block diagram in Fig. 2, and given the particular value of the gyro sensors (n=4) used in the experimental model for each of the three considered clusters, we implemented this algorithm in the Matlab/Simulink model shown in Fig. 5. Its inputs are the signals from the gyro sensors in each of the three detection clusters, while the outputs are the fusion signal (a posteriori state estimate), a posteriori estimate covariance, the variances of each of the fused gyro sensors data, and the optimal Kalman gain components. The data fusion model was considered with these outputs in order to have an easiest validation model of the redundant inertial attitude system.

To perform the experimental validation of the developed redundant attitude system, the Matlab/Simulink model in Fig. 6 was used. It integrates the data fusion algorithm for all of the three detection channels with the attitude algorithm. In the experimental test some data were simultaneously acquired from a three-dimensional redundant gyro sensors unit, especially realized for this action, and from an integrated navigator INS/GPS, both of these boarded on a testing car which played the role of the monitored vehicle. The INS/GPS system was used as reference system to evaluate the errors of our attitude angles. The three-dimensional redundant gyro sensors unit contained twelve gyros disposed in three clusters of four sensors each along the x, y and z axes of the body frame. The data acquired from the gyro clusters were further applied to the inputs of the model in Fig. 6.

The gyro sensors data in the three detection clusters and the fusion results for each cluster are shown in Fig. 7, while Fig. 8 presents the variances of this data. The upper part of Fig. 8 shows the results for gyro sensors, while the lower part presents a posteriori estimate covariance for each of the three clusters. A significant reduction of the noise level when the data fusion algorithm is used can be easily observed from Fig. 7. The decreasing of the noise level is also emphasized by the reduced values of the estimates’ covariance in comparison with the sensors’ variances given in Fig. 8. The corresponding Kalman gains for each gyro in the three clusters are depicted in Fig. 9.

Fig. 10 presents a comparative study between the attitude angle solution of our redundant attitude system and of the reference INS/GPS navigator. Also, are shown the results obtained if the attitude solution is founded by using the data from the second sensor in each of the three gyro sensors clusters included in redundant detection unit. The initial values of the attitude angles were: 0.027 deg for roll angle, 0.051 deg for pitch angle, and 108.103 deg for yaw angle.

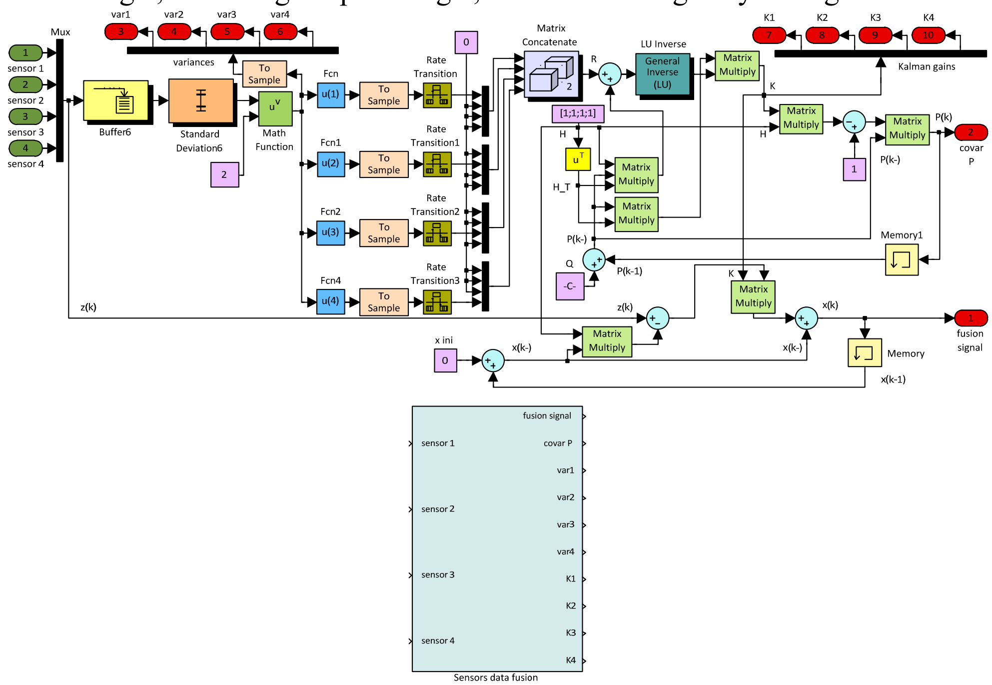

Fig. 5. Matlab/Simulink model for the fusion algorithm

The gyro sensors data in the three detection clusters and the fusion results for each cluster are shown in Fig. 7, while Fig. 8 presents the variances of this data. The upper part of Fig. 8 shows the results for gyro sensors, while the lower part presents a posteriori estimate covariance for each of the three clusters. A significant reduction of the noise level when the data fusion algorithm is used can be easily observed from Fig. 7. The decreasing of the noise level is also emphasized by the reduced values of the estimates' covariance in comparison with the sensors' variances given in Fig. 8. The corresponding Kalman gains for each gyro in the three clusters are depicted in Fig. 9.

Fig. 10 presents a comparative study between the attitude angle solution of our redundant attitude system and of the reference INS/GPS navigator. Also, are shown the results obtained if the attitude solution is founded by using the data from the second sensor in each of the three gyro sensors clusters included in redundant detection unit. The initial values of the attitude angles were: 0.027 deg for roll angle, 0.051 deg for pitch angle, and 108.103 deg for yaw angle.

The deviations between the attitude angles solution in our configuration and the reference INS/GPS navigator and between the attitude angles solution in non-redundant configuration (by using the data from the second sensor in each of the three gyro sensors clusters) and reference INS/GPS navigator are given in Fig.

11. It resulted that the maximum absolute deviations between the redundant attitude system and reference INS/GPS attitude angles founded during 180 s are: 0.0906 deg in roll angle, 0.0420 deg in pitch angle, and 0.7122 deg in yaw angle. On the other way, the same deviations, but between the attitude solution in non-redundant configuration and reference INS/GPS are: 0.2465 deg in roll angle, 0.0584 deg in pitch angle, and 1.5744 deg in yaw angle. By comparing the deviations resulted from our system with those resulted from the non-redundant configuration can be easily observed a significant improvement of the attitude angles determination accuracy brought by the proposed configuration.

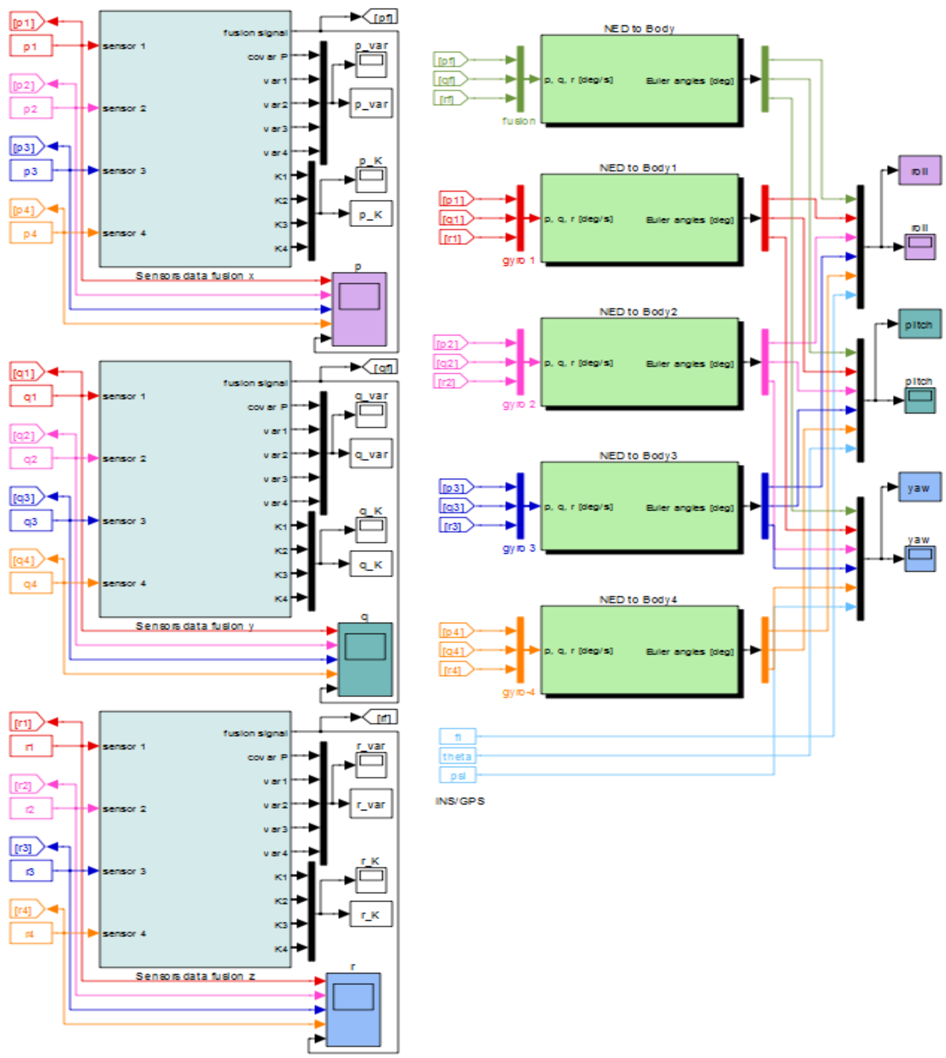

Fig. 6. Matlab/Simulink model for experimental validation

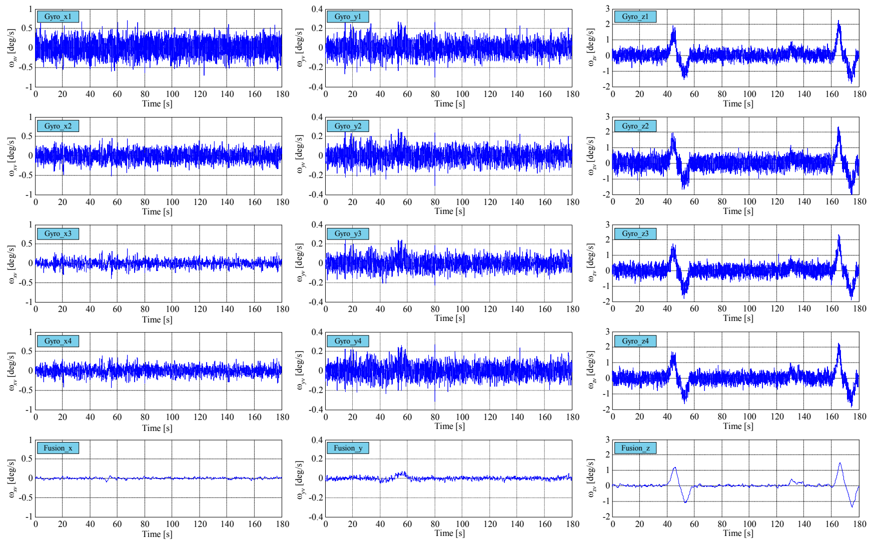

Fig. 7. Acquired data and fusion signals

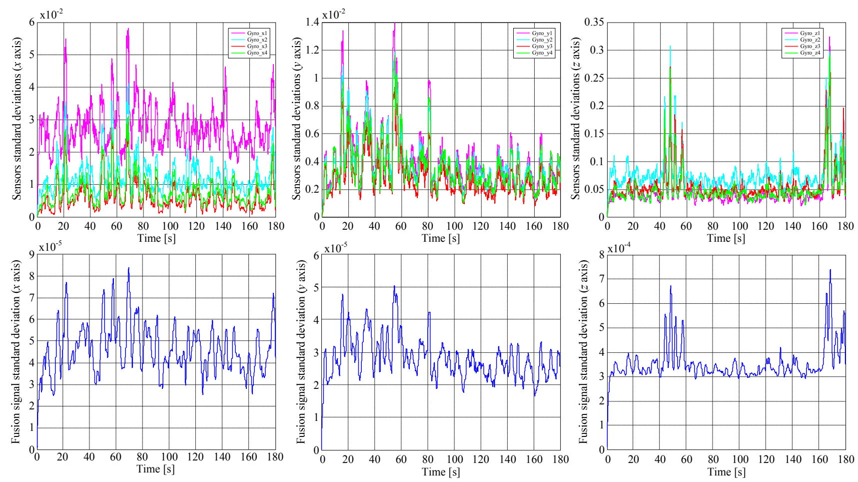

Fig. 8. Variances of sensors data and fusion signals

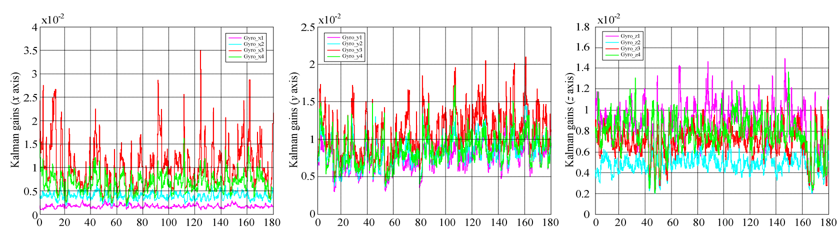

Fig. 9. Kalman gains

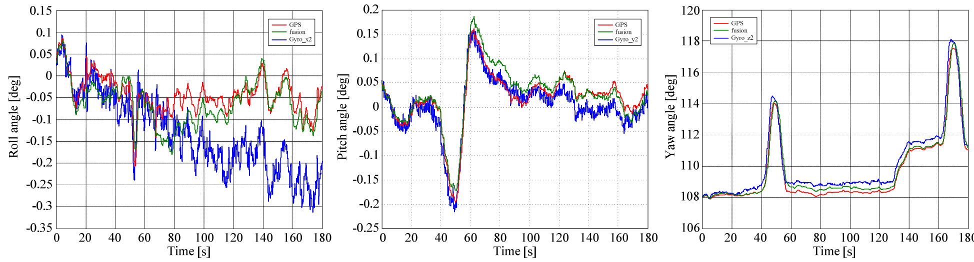

Fig. 10. Results of the experimental evaluation

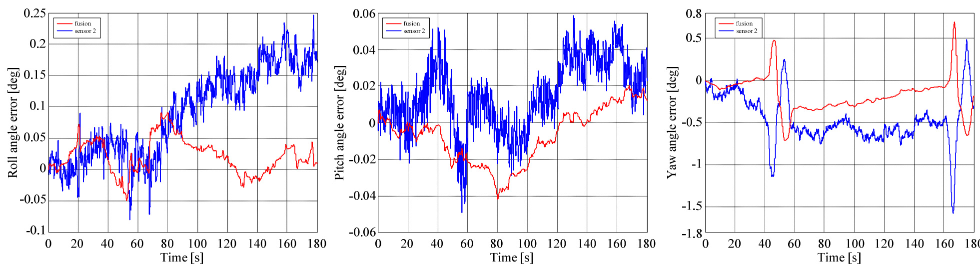

Fig. 11. Attitude angles errors

5. Conclusions

A strap-down redundant attitude system for the vehicles attitude angles determination in inertial navigation applications was here presented. The system uses the Wilcox quaternionic method to numerically integrate the Poisson quaternionic attitude equation and three redundant linear clusters of miniaturized gyro sensors. Each gyro cluster data were fused with an algorithm based on Kalman filtering concept. The mathematics of the redundant attitude system was software implemented by using the Matlab/Simulink package and experimentally validated. In the experimental test some data were simultaneously acquired from a three-dimensional redundant gyro sensors unit, especially realized for this action, and from an integrated navigator INS/GPS, both of these boarded on a testing car which played the role of the monitored vehicle. The INS/GPS system was used as reference system to evaluate the errors of our attitude angles. The experimental test confirmed a significant improvement of the attitude angles determination accuracy brought by the proposed configuration comparatively with the case when a non-redundant configuration is used.

Acknowledgements

[1] This work was supported by the Project POSDRU/88/1.5/S/61178.

[2] This work was supported by CNCSIS-UEFISCDI, project PN II-RU, No. 1/28.07.2010, “High-precision strap-down inertial navigators, based on the connection and adaptive integration of the nano and micro inertial sensors in low cost networks, with a high degree of redundance”, code TE_102/2010.

R E F E R E N C E S

[1] Savage P.G. Strapdown Inertial Navigation. Plymouth, MN, USA, Inc. 1990.

[2] Stovall S.H. Basic Inertial Navigation. Naval Air Warfare Center Weapons Division, China Lake, September, 1997.

[3] Chatfield A.B. Fundamentals of High Accuracy Inertial Navigation, American Institute of Aeronautics and Astronautics, 1997.

[4] Salychev O.S. Inertial Systems in Navigation and Geophysics. Bauman MSTU Press, Moscow, 1998.

[5] Titterton D. H., and Weston J., Strapdown inertial navigation technology - 2nd Edition, IET, 2004.

[6] Grigorie L.T. Strap-Down Inertial Navigation Systems, Ed. Sitech, Craiova, 2007.

[7] Bekir E. Introduction to Modern Navigation Systems. World Scientific Publishing Co. Pte. Ltd., 2007.

[8] Farrell J. Aided Navigation. GPS with High Rate Sensors. McGraw-Hill, 2008.

[9] Grigorie T.L., Lungu M., Edu I.R., Obreja R. Influences of the miniaturised inertial sensors errors on the navigation solution in a bidimensional SDINS in vertical plane, COMEC2011, 20-22 October, Brasov, Romania, 2011.

[10] Grigorie T.L. & Sandu, D.G. The influences of the gyro sensors' errors on the attitude calculus. ELMAR-2007, Zadar, Croatia, 12-14 September, pp. 85-92, 2007.

[11] Moody L. Sensors, Measurement Fusion and Missile Trajectory Optimisation, PhD Thesis, Cranfield University, Department of Aerospace, July 2003, UK.

[12] Schmidt G. INS/GPS Technology Trends, RTO-EN-SET-116, Low-Cost Navigation Sensors and Integration Technology, March 2010.

[13] Barbour N., Hopkins R., Kourepenis A. & Ward P. Inertial MEMS System Applications, NATO RTO Lecture Series, RTO-EN-SET-116, Low-Cost Navigation Sensors and Integration Technology, March 2010.

[14] Hopkins R.E., Barbour N., Gustafson D.E. & Sherman P. Miniature Inertial and Augmentation Sensors for Integrated Inertial/GPS Based Navigation Applications, NATO RTO Lecture Series, RTO-EN-SET-116, Low-Cost Navigation Sensors and Integration Technology, March 2010.

[15] Barbour N. Inertial Navigation Sensors, RTO-EN-SET-116, Low-Cost Navigation Sensors and Integration Technology, March 2010.

[16] Edu I.R., Obreja R., Grigorie T.L. Current technologies and trends in the development of gyros used in navigation applications – a review, Conference on Communications and Information Technology (CIT-2011), July, 14-16, Corfu, Greece, pp. 63-68, 2011.

[17] Edu I.R., Obreja R., Grigorie T.L. Miniaturised accelerometers architectures, development technologies and applications, International Multidisciplinary Scientific GeoConference & EXPO – SGEM 2011, 19-25 June, Albena, Bulgaria, 2011.

[18] Edu I.R., Grigorie T.L., Cepisca C. Kalman filtering of the miniaturized inertial sensors' data for inertial navigation, The 7th International Symposium on Advanced Topics in Electrical Engineering (ATEE), May 12-15, Bucharest, Romania, pp. 1-6, 2011.

[19] Grigorie, T.L., Lungu, M., Edu, I.R., Obreja R. A tool for the aircrafts attitude determination, International Conference NAV-MAR_EDU – 2011, November 11-13, Constanta, Romania, 2011.

[20] Radix J.C. Systèmes inertiels a composants lies <<Strap-Down>>, Cepadues-Editions, Ecole Nationale Supérieure de l'Aéronautique et de l'Espace SUP'AERO, Toulouse, 1993.